Eur. J. Mineral.
2007, **19**, 15–27

Order and anti-order in olivine III: Variation of the cation distribution in the Fe,Mg olivine solid solution series with temperature and composition

ROLF HEINEMANN[1], HERBERT KROLL[1,*], ARMIN KIRFEL[2] and BRUNO BARBIER[2]

[1]Institut für Mineralogie, Westfälische Wilhelms-Universität, Corrensstr. 24, 48149 Münster, Germany
*Corresponding author, e-mail: kroll@nwz.uni-muenster.de
[2]Mineralogisch-Petrologisches Institut, Poppelsdorfer Schloss, 53115 Bonn, Germany

Abstract: The structures of four Fe,Mg olivine crystals Fa11.6, Fa22.3, Fa27.6 and Fa27.8 have been investigated by *ex situ* and *in situ* experiments using single-crystal X-ray diffractometry. For the *ex situ* experiments, the crystals were quenched after equilibration at temperatures between 500 °C and 900 °C. Resetting effects were only observed for samples quenched from 900 °C. The *in situ* experiments were performed at temperatures up to 750 °C. With increasing equilibration temperature, Fe^{2+} was found to progressively segregate into the octahedral M1 site, *i.e.* the degree of anti-order increases with rising temperature. Thus, contrary to the results of Rinaldi *et al*. (2000) and Redfern *et al*. (2000), no indication of an ordering reversal at high temperatures is found. Incorporation of the results of Heinemann *et al*. (2006) on olivine Fa47.9 into the present study allows for the first time to systematically investigate the compositional variation of the temperature dependence of the Fe^{2+},Mg site occupancies. The formulation of Thompson (1969, 1970) for solid solutions undergoing non-convergent disordering processes,

$$-RT\ln K_D = [\Delta H^0_{exch} - (L^H_{M1} - L^H_{M2})X] - T[\Delta S^0_{exch} - (L^S_{M1} - L^S_{M2})X], \quad (1)$$

yielded

$\Delta H^0_{exch} = 1153\ (\pm 67)$ J/mol $\Delta S^0_{exch} = 3.743(\pm 0.072)$ J/molK
$L^H_{M1} - L^H_{M2} = 973\ (\pm\ 211)$ J/mol $L^S_{M1} - L^S_{M2} = -0.89\ (\pm\ 0.24)$ J/molK.

ΔH^0_{exch} and ΔS^0_{exch} are the exchange enthalpy and entropy, respectively, related to the Fe^{2+},Mg site exchange, $L^H_{M1,M2}$ and $L^S_{M1,M2}$ denote enthalpic and entropic intrasite interaction parameters. The compositional parameter X varies between –1 for forsterite (Fa0) and +1 for fayalite (Fa100). The magnitudes and signs of the four refined quantities can be rationalized in terms of thermodynamic and crystal-chemical considerations. $(L^H_{M1} - L^H_{M2}) > 0$ indicates that the interactions between the M1 sites are stronger than those between the M2 sites, conforming with the M1-M1 distances being shorter than the M2-M2 distances. $(L^S_{M1} - L^S_{M2}) < 0$ relates to the electronic entropy which is proportional to the Fa-content. According to equation (1), ΔH^0_{exch} increases towards the Mg endmember while ΔS^0_{exch} decreases. Since $\Delta H^0_{exch} > 0$ stabilizes the *ordered* state whereas $\Delta S^0_{exch} > 0$ stabilizes the *anti-ordered* state, it follows that the ordered state is progressively favoured with increasing Mg content. Consequently, ordered site distributions should occur only in slowly cooled Mg-rich olivines, whereas olivines with Fa > 25 mol% should be found in their anti-ordered states frozen during cooling. This conclusion is supported by structure refinements and ordering path simulations for a metamorphic olivine Fa12.4 as well as two volcanic olivines Fa25.6 and Fa27.8.

Key-words: olivine, order, anti-order, cation distribution, non-convergent disordering, solid solution, geospeedometry.

Introduction

In the recent literature, the temperature variation of the Fe^{2+},Mg cation distribution in olivine, $Mg_2[SiO_4]$ (Fo) – $Fe_2[SiO_4]$ (Fa), has experienced a controversial discussion. Redfern *et al*. (2000) reported that Fe^{2+} in olivine of composition Fa50, after an initial slight preference for the M1 site, significantly segregates into the M2 site as soon as the temperature exceeds 650 °C. Artioli *et al*. (1995) and Rinaldi *et al*. (2000) found a similar behaviour in Fa10 and Fa12 for which they observed the same effect at about 850 °C. In contrast, Morozov *et al.* (2001, 2002, 2005), based on Mößbauer spectroscopy on quenched Fa50 samples, could not confirm such behaviour. Their findings agree with those of Heinemann *et al*. (2003a,b, 2006) who observed in both *ex situ* and *in situ* single-crystal X-ray diffraction experiments performed on Fa47.9 up to 900 °C that Fe^{2+} continues to fractionate into the M1 site with increasing temperature.

In the present study, we extend these investigations by reporting on the temperature variation of the Fe^{2+},Mg cation distribution in three Mg-rich olivines with compositions Fa22.3, Fa27.6 and Fa27.8, and, in completion of earlier in-

DOI: 10.1127/0935-1221/2007/0019-0015
0935-1221/07/0019-0015 $ 5.85

vestigations, in two olivines, Fa11.6, from the Acapulco meteorite. In addition, the site occupancies of two untreated metamorphic and volcanic olivines with 12.4% and 25.6% Fa content, respectively, have also been determined in order to investigate the evolution of site occupancies under the conditions of both slow and fast cooling.

Experimental methods

Electron microprobe analysis

(1) The two meteoritic olivine crystals Fa11.6 derive from a previous study by Heinemann *et al*. (1999) where details of the microprobe analysis are given. (2) The four olivine phenocrysts with compositions Fa22.3, Fa25.6, Fa27.6 and Fa27.8 were separated from a hand-specimen of an andesitic lava flow from the Saar-Nahe basin, Germany (Schmidt-Riegraf, 1996). After cutting the phenocrysts into smaller pieces, we have chosen one single-crystal of each phenocryst for further X-ray investigation. All crystals were free of inclusions, showed distinct extinctions under the polarizing microscope and produced sharp diffraction spots on Laue photographs. Prior to their X-ray investigations, the four single-crystals were ground and polished for chemical analyses with the electron microprobe (JEOL Superprobe JXA-8600 MX operated by S. Matveev, Münster). According to the data reduced by the ZAF correction technique, all crystals proved to be homogeneous. The mean values of 26 to 80 point analyses on each crystal are reported in Tab. 1 showing that the crystal-chemical constraints, (i) sum over positive valences = 8, (ii) sum over tetrahedral plus octahedral cations = 3, are satisfactorily met. Deviations from the constraints were accounted for following Ganguly *et al*. (1994). (3) Another olivine crystal (Fa12.4) was selected from a granulite-facies marble from South Madagascar and treated as described above (microprobe operator: M. Enders, Münster).

In situ and *ex situ* experiments

As in part I of this series (Heinemann *et al*., 2006), the single-crystal structure refinements were carried out with two groups of X-ray intensity data collected on a conventional and a rotating anode diffractometer operated in Münster and Bonn, respectively. These groups are therefore referred to as (MS) and (BN). The (MS)-data were measured at ambient temperatures on crystals that had been rapidly quenched to room temperature after annealing between 500 °C and 900 °C (*ex situ* experiments). For the annealing experiments, the crystals were inserted into silica glass capillaries which were then placed into silica glass tubes containing Fe/FeO mixtures to control the oxygen fugacity.

The (BN)-data were collected *in situ* at elevated temperatures using a N_2 gas stream device to heat the crystals mounted in sealed silica glass capillaries filled with a CO/CO_2 gas mixture which provided an oxygen fugacity corresponding to the Fe/FeO buffer. The heating device, its performance and in particular the method of temperature assessment are described by Scheufler *et al.* (1997). Further information on the (MS) and (BN) preparation techniques is given in Heinemann *et al*. (2006).

The annealing temperatures, *in situ* temperatures and run times are compiled in Tab. 2.

Data collection and reduction

The room temperature X-ray intensity data (MS) were collected on an ENRAF-NONIUS-CAD4 four-circle diffractometer using MoKα-radiation monochromatized by a pyrolytic graphite crystal. Covering the octants hkl, $\overline{h}$kl, $\overline{h}\overline{k}$l, and hk$\overline{l}$ data were measured up to $\sin(\theta)/\lambda = 1.08$ Å^{-1} using an ω–2θ scan mode optimized for each run. The *in situ* measurements (BN) were performed on a rotating Mo-anode diffractometer, RIGAKU AFC6, also equipped with a pyrolytic graphite monochromator. Due to the gas stream heater the data collection was limited to $\sin(\theta)/\lambda = 0.70$ Å^{-1}. As for MS, the intensities were measured for half spheres. The respective data reductions followed the procedures described by Heinemann *et al*. (2006). For details about both data collections and reductions, see Table 2.

Structure refinement

All structure refinements were carried out in space group *Pbnm* using the program RFINE 90, a version of RFINE4 updated by Finger & Prince (1975) and locally modified by R. Heinemann. Atomic scattering factors were taken from Cromer & Waber (1974) and Hovestreydt (1983), anomalous dispersion corrections from Doyle & Turner (1968). A partially ionic structure model was used in which the metal atoms were considered fully ionized whereas silicon and oxygen were assumed partially ionic, Si^{2+} and $O^{1.5-}$, respectively. The large Ca and Mn cations were assigned to the M2 site. Fe^{2+} and Mg were free to fractionate between M1 and M2, subject to the site occupancy constraints

$$X^{M1}_{Fe} + X^{M1}_{Mg} = 1$$

$$X^{M2}_{Fe} + X^{M2}_{Mg} = 1 - X^{M2}_{Ca} - X^{M2}_{Mn}, \quad (2)$$

and the chemical constraint

$$X^{M1}_{Fe} + X^{M2}_{Fe} = \text{constant (see Table 1)}. \quad (3)$$

$X^{site}_{element}$ denotes the amount of Fe^{2+} or Mg occupying the M1 or M2 site, respectively. In the refinements, the observed structure amplitudes $|F_o|$ were weighted according to $w = [\sigma^2(F_o) + (\frac{1}{2}R_i \cdot F_o)^2]^{-1}$ subject to the robust/resistant technique. R_i is the internal agreement of the data based on $|I_{obs}|$ (*e.g.*, Le Hénaff *et al.*, 1997). An isotropic extinction coefficient was refined according to Becker & Coppens (1974; type I, Lorentzian mosaic distribution), this however only in the final stages of the refinements due to high correlation with the scale factor.

Table 1. Electron microprobe analyses of volcanic Saar-Nahe (CSR) and metamorphic South Madagascar (Ro8/2) olivines.

CSR –1	oxides	observed	sigma[a]	atoms	observed	sigma[a]	adjusted
	SiO_2	37.244	0.166	Si	0.9820	0.0044	1.0000
	MgO	36.824	0.222	Mg	1.4475	0.0087	1.4320
	FeO	25.402	0.316	Fe^{2+}	0.5601	0.0070	0.5518
	MnO	0.406	0.063	Mn	0.0091	0.0014	0.0087
	CaO	0.267	0.018	Ca	0.0075	0.0005	0.0075
	sum total	100.143			3.0062		3.0000
	Σval				7.9764		8.0000
	Δ(M-T)[b]				0.1204		0.0000
	X_{Fa}[c]						0.2782
CSR –2	oxides	observed	sigma[a]	atoms	observed	sigma[a]	adjusted
	SiO_2	38.410	0.294	Si	0.9926	0.0076	1.0000
	MgO	40.342	0.349	Mg	1.5542	0.0134	1.5442
	FeO	20.678	0.495	Fe^{2+}	0.4469	0.0107	0.4437
	MnO	0.321	0.077	Mn	0.0070	0.0017	0.0070
	CaO	0.189	0.031	Ca	0.0052	0.0009	0.0052
	sum total	99.940			3.0059		3.0001
	Σval				7.9970		8.0002
	Δ(M-T)[b]				0.0562		0.0002
	X_{Fa}[c]						0.2232
CSR –5	oxides	observed	sigma[a]	atoms	observed	sigma[a]	adjusted
	SiO_2	38.082	0.211	Si	0.9917	0.0029	1.0000
	MgO	38.104	0.239	Mg	1.4793	0.0078	1.4774
	FeO	23.504	0.261	Fe^{2+}	0.5119	0.0051	0.5092
	MnO	0.349	0.040	Mn	0.0077	0.0009	0.0076
	CaO	0.209	0.015	Ca	0.0058	0.0004	0.0058
	sum total	100.248			2.9964		3.0000
	Σval				7.9762		8.0000
	Δ(M-T)[b]				0.0426		0.0000
	X_{Fa}[c]						0.2563
CSR –12	oxides	observed	sigma[a]	atoms	observed	sigma[a]	adjusted
	SiO_2	37.741	0.228	Si	0.9921	0.0060	1.0000
	MgO	36.640	0.264	Mg	1.4358	0.0103	1.4354
	FeO	25.102	0.386	Fe^{2+}	0.5518	0.0085	0.5483
	MnO	0.405	0.060	Mn	0.0090	0.0013	0.0089
	CaO	0.264	0.017	Ca	0.0074	0.0005	0.0074
	sum total	100.152			2.9961		3.0000
	Σval				7.9764		8.0000
	Δ(M-T)[b]				0.0396		0.0000
	X_{Fa}[c]						0.2764
Ro 8/2	oxides	observed	sigma[a]	atoms	observed	sigma[a]	adjusted
	SiO_2	39.828	0.185	Si	0.9916	0.0046	1.0000
	MgO	46.223	0.335	Mg	1.7156	0.0124	1.7163
	FeO	11.669	0.122	Fe^{2+}	0.2430	0.0025	0.2436
	MnO	1.869	0.036	Mn	0.0394	0.0008	0.0395
	CaO	0.023	0.010	Ca	0.0006	0.0003	0.0006
	sum total	99.612			2.9902		3.0000
	Σval				7.9636		8.0000
	Δ(M-T)[b]				0.0308		0.0000
	X_{Fa}[c]						0.1243

[a] sigma: estimated standard deviation
[b] Δ(M-T): difference between charge excess in the M sites and charge deficiency in the T sites
[c] $X_{Fa} = Fe / (Fe+Mg)$, $X_{Fo} = 1 - X_{Fa}$

Table 2. Thermal treatment of the samples; data collection and reduction parameters.

data set				T (°C)	annealing time	type of measurement	max. $\sin\theta/\lambda$ ($Å^{-1}$)	No. of unique refl.	internal R ($\|I_{abs}\|$)
MS	Fa 12.4	Ro	–8/2	as is	–	RT[(1)]	1.09	1688	0.012
MS	Fa 11.6	Aca	–7–1	as is	–	RT	1.09	1612	0.023
			–7–2	750	4 d	*ex situ*[(2)]	1.09	1684	0.019
			–7–3	650	6 d	*ex situ*	1.09	1684	0.029
			–7–4[(3)]	500	26 d	*ex situ*	1.09	1684	0.030
			–7–5	550	131 d	*ex situ*	1.09	1684	0.020
			–7–6	600	20 d	*ex situ*	1.09	1684	0.029
			–7–7	700	5 d	*ex situ*	1.09	1684	0.026
MS	Fa 11.6	Aca	–8–1	as is	–	RT	1.09	1684	0.017
			–8–2	750	4 d	*ex situ*	1.09	1684	0.020
			–8–3	650	6 d	*ex situ*	1.09	1684	0.021
			–8–4	500	26 d	*ex situ*	1.09	1684	0.026
			–8–5	550	131 d	*ex situ*	1.09	1684	0.022
			–8–6	600	20 d	*ex situ*	1.09	1684	0.026
			–8–7	700	5 d	*ex situ*	1.09	1686	0.024
BN	Fa 22.3	CSR	–2–1	20	–	*in situ*	0.70	346	0.021
			–2–2	450	4 h	*in situ*	0.70	348	0.013
			–2–3	600	4 d	*in situ*	0.70	354	0.024
			–2–4	677	2 d	*in situ*	0.70	356	0.024
			–2–5	725	2.5 h	*in situ*	0.70	357	0.024
			–2–6	800	2.5 h	*in situ*	0.70	358	0.023
MS	Fa 25.6	CSR	–5–1	as is	–	RT	1.09	1704	0.017
MS	Fa 27.6	CSR	–12–1	625	7 d	*ex situ*	1.09	1704	0.018
			–12–2	700	4 d	*ex situ*	1.09	1703	0.018
			–12–3	550	40 d	*ex situ*	1.09	1704	0.021
			–12–4	900	1 d	*ex situ*	1.09	1704	0.017
MS	Fa 27.8	CSR	–1–1	as is	–	RT	1.09	1704	0.021
			–1–2	625	7 d	*ex situ*	1.09	1704	0.016
			–1–3	700	4 d	*ex situ*	1.09	1703	0.019
			–1–4	550	40 d	*ex situ*	1.09	1704	0.016
			–1–5	900	1 d	*ex situ*	1.09	1703	0.014

Notes: (1) RT = room temperature. (2) *ex situ* = data collection at ambient conditions after quench of the sample from the indicated temperature where it had been annealed for the time given in column 3. (3) Prior to its isothermal annealing for 26 d at 500 °C the sample Aca-7-4 had been slowly cooled from 625 °C to 300 °C. During this process its Fe^{2+},Mg site distribution became frozen in close to 500 °C so that further annealing for a relatively short time at this temperature was sufficient for the crystal to reach equilibrium.

Results and discussion

Variation with temperature and composition of the Fe^{2+},Mg site occupancies

Detailed results of the structure refinements are listed in Tab. 3, Tab. 4 and Tab. 5. The unit-cell dimensions are given in Tab. 6. With K_D defined as

$$K_D = X_{Fe}^{M1} X_{Mg}^{M2} / X_{Fe}^{M2} X_{Mg}^{M1} \quad (4)$$

the ensuing $\ln K_D$ values of the olivines Fa11.6, Fa22.3, Fa27.6 and Fa27.8 are plotted versus 1/T in Fig. 1 which additionally shows the results of Fa47.9 reported by Heinemann *et al*. (2006).

At the lowest temperature of equilibration (500 °C), Fe^{2+} is slightly enriched in M1, the site into which it continues to fractionate, increasing the degree of anti-order with increasing temperature. Hence, the slope of each $\ln K_D$ line is negative, and $\ln K_D > 0$ for all experimental temperatures. With decreasing Fa content, the slope becomes slightly steeper. Its dependence on the Fe,Mg composition can be modelled in terms of Thompson's (1969, 1970) formulation of the order induced Gibbs energy, G^{ord}, which for olivine can be written as (Kroll *et al*., 2006)

$$G^{ord} = G_Q - G_{Q=0} = -\frac{1}{2}\left[\Delta G^0_{exch} - (L^G_{M1} - L^G_{M2})\, X\right] Q - TS^{ord}_{conf} \quad (5)$$

where the compositional variable X,

$$X = 2X_{Fa} - 1, \quad (6)$$

takes values between –1 (forsterite, Fa0) and +1 (fayalite, Fa100). The long range order parameter Q,

$$Q = X_{Fe^{2+}}^{M2} - X_{Fe^{2+}}^{M1}, \quad (7)$$

is –1 and +1 for the fully anti-ordered (Fe^{2+} in M1, Mg in M2) and fully ordered state (Mg in M1, Fe^{2+} in M2), respectively. ΔG^0_{exch} expresses the Gibbs energy difference between the anti-ordered and ordered states

$$\Delta G^0_{exch} = G^0_{Q=-1} - G^0_{Q=1}. \quad (8)$$

The linear X term in which L^G_{M1} and L^G_{M2} account for intrasite interactions adds a composition dependent energy contribution to ΔG^0_{exch}. S^{ord}_{conf} is the conventional configurational entropy due to ordering. Since at internal equilibrium $\partial G^{ord}/\partial Q = 0$, one obtains

$$\begin{aligned} -RT\ln K_D &= \Delta G^0_{exch} - (L^G_{M1} - L^G_{M2})\,X \\ &= [\,\Delta H^0_{exch} - (L^H_{M1} - L^H_{M2})X] \\ &\quad - T[\,\Delta S^0_{exch} - (L^S_{M1} - L^S_{M2})X]\,. \end{aligned} \quad (9)$$

With the exception of Fa22.3 all $\ln K_D$ data shown in Fig. 1 were used to obtain the adjustable parameters of equation (9), *i.e.* ΔH^0_{exch}, ΔS^0_{exch}, $(L^H_{M1} - L^H_{M2})$ and $(L^S_{M1} - L^S_{M2})$, by weighted least-squares analysis. The refined parameters served in turn to calculate the $\ln K_D$ lines plotted in Fig. 1, which thus are not regression lines obtained for the individual samples but lines derived from a general model. The agreement with the experimental $\ln K_D$ values is convincing, particularly for Fa47.9 where both *in situ* and *ex situ* data are combined. The $\ln K_D$ data of Fa22.3 were not included in the regression because they are considered less reliable than the other data. This is most probably due to the fact that reflection intensities could be collected in only four rather than eight octants (as for Fa47.9) and this for technical reasons only up to $\sin(\theta/\lambda) = 0.70$ Å^{-1} rather than to 1.08 Å^{-1} (as for the *ex situ* experiments). Nevertheless, the Fa22.3 results are included into Fig. 1 for comparison. The symbol drawn at 625 °C represents in fact two equal results obtained at 20 °C and 450 °C, respectively, but were assigned to the temperature of the prior equilibration since a redistribution of the cations during the time of data collection is unlikely up to 450 °C.

The results of the least-squares analysis, *i.e.*,

$$\begin{aligned} &\Delta H^0_{exch} = 1153\ (\pm\ 67)\ \text{J/mol} \\ &\Delta S^0_{exch} = 3.743(\pm\ 0.072)\ \text{J/molK} \\ &L^H_{M1} - L^H_{M2} = 973\ (\pm\ 211)\ \text{J/mol} \\ &L^S_{M1} - L^S_{M2} = -0.89\ (\pm\ 0.24)\ \text{J/molK} \end{aligned} \quad (10)$$

deserve a discussion of their thermodynamic and crystal-chemical implications.

(1) ΔH^0_{exch} and ΔS^0_{exch} relate to the exchange of one mole of Fe^{2+} on M2 with one mole of Mg on M1. For X = 0 (Fa50), ΔH^0_{exch} and ΔS^0_{exch} take the values given in equation (10). Within error limits, these values reproduce those reported by Kroll *et al*. (2006), ΔH^0_{exch} = 1164(54) J/mol and ΔS^0_{exch} = 3.68(6) J/molK, for a crystal with X ≈ 0 (Fa47.9) indicating that the dependence of the exchange parameters on composition is adequately modelled by equation (9).

The exchange enthalpy that Redfern *et al*. (2000) derived from their experiments, –11100 J/molK, strongly contrasts to our value with regard to both size and sign (note the sign error associated with the value quoted by the authors). In a $\ln K_D$ vs. 1/T diagram, ΔH^0_{exch} = –11100 J/molK indicates a steep, positively sloping line, whereas we found the slope to be gentle and negative (Fig. 1).

(2) Both ΔH^0_{exch} and ΔS^0_{exch} are positive with ΔH^0_{exch} being small. This has interesting consequences with respect to the temperature and composition dependent attainment of ordered and anti-ordered states. A brief account is given further below; for a detailed discussion of the crystal-chemical factors that govern the magnitudes and signs of ΔH^0_{exch} and ΔS^0_{exch} in AB olivines, see Kroll *et al*. (2006).

(3) The compositional variation of the exchange enthalpy is controlled by the magnitude and sign of the difference between L^H_{M1} and L^H_{M2}. Since $(L^H_{M1} - L^H_{M2}) > 0$, the exchange enthalpy increases with decreasing X, *i.e.* towards the Mg endmember (X = –1), *vice versa* it decreases towards the Fe endmember (X = 1),

$$\Delta H^0_{exch}(X) = \Delta H^0_{exch}\ (X = 0) - (L^H_{M1} - L^H_{M2})\,X. \quad (11)$$

The larger the (positive) value of $\Delta H^0_{exch}(X)$, the smaller is the enthalpy of the ordered state relative to that of the anti-ordered state. Thus, the ordered state becomes the more favoured the larger the Mg content. This has in fact been confirmed by the investigation of Mg-rich metamorphic olivines (Aikawa *et al.*, 1985; Princivalle, 1990; Freiheit *et al.*, 2000; and this study), in which due to slow cooling the cation exchange processes could proceed down to low temperatures. In such case, the energy $T\Delta S^0_{exch}(X)$ becomes sufficiently small relative to $\Delta H^0_{exch}(X)$ so that an ordered state ($\ln K_D < 0$) is attained, contrary to the regime of higher temperatures at which anti-order prevails ($\ln K_D > 0$) due to the dominance of $T\Delta S^0_{exch}(X)$ (see Fig. 1).

The quantities L^H_{M1} and L^H_{M2} model energetic interactions between the cations on the M1 and M2 sites, respectively. Neither of them is likely to be negative since in analogy to

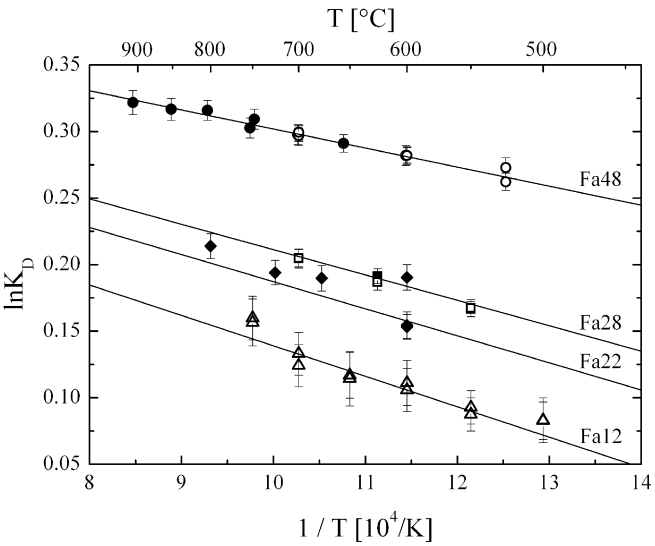

Fig. 1. Variation of $\ln K_D$ with inverse temperature and composition of olivines Fa11.6, Fa22.3, Fa27.6 and Fa27.8 (Table 5) and Fa47.9 (Heinemann *et al.*, 2006). Open symbols: *ex situ* measurements, full symbols: *in situ* measurements. K_D is defined as $K_D = X^{M1}_{Fe} X^{M2}_{Mg} / X^{M2}_{Fe} X^{M1}_{Mg}$ where the site occupancies are indicated by $X^{site}_{element}$. Fa22.3 was quenched from equilibration at 625 °C. Therefore, measurements at 20 °C and 450 °C yielded site occupancies that correspond to 625 °C (or nearly so) as plotted.

Table 3. Atomic fractional coordinates and anisotropic thermal displacement parameters [Å^2] of Saar-Nahe olivine CSR-2 (Fa22.3), obtained from refinements with *in situ* data (BN-data).

sample		CSR-2	CSR-2	CSR-2	CSR-2	CSR-2	CSR-2
T [°C]		20	450	600	677	725	800
Si	x	0.42722 (10)	0.42728 (10)	0.42731 (10)	0.42740 (10)	0.42745 (9)	0.42740 (9)
	y	0.09491 (5)	0.09495 (5)	0.09497 (5)	0.09498 (5)	0.09496 (4)	0.09503 (4)
	U_{11}	0.0046 (2)	0.0080 (3)	0.0096 (2)	0.0104 (2)	0.0110 (2)	0.0117 (2)
	U_{22}	0.0068 (2)	0.0122 (2)	0.0143 (2)	0.0156 (2)	0.0163 (2)	0.0175 (2)
	U_{33}	0.0055 (2)	0.0106 (3)	0.0128 (2)	0.0139 (2)	0.0148 (2)	0.0160 (2)
	U_{12}	0.0001 (2)	0.0002 (2)	0.0002 (2)	0.0003 (2)	0.0004 (2)	0.0004 (2)
M1	X_{Fe}	0.2364 (8)	0.2365 (9)	0.2396 (8)	0.2395 (8)	0.2399 (8)	0.2416 (8)
	U_{11}	0.0057	0.0119	0.0146	0.0162	0.0171	0.0187
	U_{22}	0.0097	0.0207	0.0253	0.0278	0.0295	0.0321
	U_{33}	0.0054	0.0118	0.0145	0.0160	0.0170	0.0186
	U_{12}	0.0001	–0.0002	–0.0004	–0.0004	–0.0005	–0.0006
	U_{13}	–0.0006	–0.0017	–0.0022	–0.0026	–0.0028	–0.0031
	U_{23}	–0.0013	–0.0035	–0.0043	–0.0048	–0.0051	–0.0056
M2	X_{Fe}	0.2073 (8)	0.2072 (9)	0.2041 (8)	0.2042 (8)	0.2038 (8)	0.2021 (8)
	x	0.98864 (9)	0.98937 (10)	0.98987 (10)	0.98997 (10)	0.99009 (9)	0.99027 (9)
	y	0.27808 (4)	0.27877 (5)	0.27906 (4)	0.27916 (5)	0.27928 (4)	0.27942 (4)
	U_{11}	0.0077	0.0156	0.0190	0.0209	0.0221	0.0241
	U_{22}	0.0066	0.0129	0.0157	0.0172	0.0182	0.0198
	U_{33}	0.0060	0.0136	0.0170	0.0188	0.0200	0.0219
	U_{12}	0.0001	0.0004	0.0005	0.0006	0.0006	0.0007
O1	x	0.76600 (26)	0.76479 (29)	0.76432 (27)	0.76414 (26)	0.76399 (26)	0.76384 (26)
	y	0.09183 (11)	0.09203 (12)	0.09212 (11)	0.09209 (11)	0.09213 (11)	0.09216 (11)
	U_{11}	0.0050 (6)	0.0087 (6)	0.0108 (6)	0.0117 (6)	0.0128 (6)	0.0136 (6)
	U_{22}	0.0094 (6)	0.0184 (7)	0.0219 (6)	0.0241 (6)	0.0253 (6)	0.0274 (6)
	U_{33}	0.0051 (5)	0.0120 (6)	0.0146 (6)	0.0165 (6)	0.0173 (6)	0.0194 (6)
	U_{12}	0.0002 (5)	0.0000 (5)	0.0001 (5)	–0.0002 (5)	0.0000 (5)	–0.0001 (5)
O2	x	0.21854 (24)	0.21830 (27)	0.21869 (25)	0.21821 (25)	0.21813 (24)	0.21813 (24)
	y	0.44857 (11)	0.44934 (12)	0.44963 (11)	0.44983 (11)	0.44995 (11)	0.45016 (10)
	U_{11}	0.0068 (5)	0.0129 (6)	0.0155 (6)	0.0171 (6)	0.0178 (6)	0.0196 (6)
	U_{22}	0.0065 (6)	0.0117 (6)	0.0142 (6)	0.0151 (6)	0.0155 (6)	0.0170 (6)
	U_{33}	0.0064 (6)	0.0140 (7)	0.0166 (6)	0.0189 (6)	0.0204 (6)	0.0220 (6)
	U_{12}	–0.0002 (5)	–0.0005 (6)	–0.0004 (5)	–0.0002 (5)	–0.0003 (5)	0.0000 (5)
O3	x	0.27999 (18)	0.28146 (20)	0.28200 (18)	0.28231 (18)	0.28263 (18)	0.28300 (18)
	y	0.16359 (8)	0.16339 (8)	0.16333 (7)	0.16336 (7)	0.16341 (7)	0.16338 (7)
	z	0.03428 (13)	0.03537 (14)	0.03556 (14)	0.03580 (14)	0.03599 (13)	0.03619 (13)
	U_{11}	0.0055 (4)	0.0120 (5)	0.0147 (4)	0.0162 (4)	0.0172 (4)	0.0188 (4)
	U_{22}	0.0092 (4)	0.0176 (4)	0.0210 (4)	0.0230 (4)	0.0243 (4)	0.0265 (4)
	U_{33}	0.0073 (4)	0.0140 (5)	0.0164 (4)	0.0180 (4)	0.0192 (4)	0.0207 (4)
	U_{12}	0.0000 (3)	0.0003 (4)	0.0006 (4)	0.0005 (4)	0.0008 (4)	0.0008 (4)
	U_{13}	–0.0003 (4)	–0.0007 (4)	–0.0008 (4)	–0.0008 (4)	–0.0011 (4)	–0.0008 (4)
	U_{23}	0.0014 (3)	0.0035 (4)	0.0049 (4)	0.0055 (4)	0.0058 (4)	0.0064 (4)

Note: Special positions not listed above: x(M1) = y(M1) = z(M1) = 0, z(Si) = z(M2) = z(O1) = z(O2) = ¼.

solid solution theory, negative values would suggest ordering tendencies *within* each of the two sublattices whereas exchange *between* the sublattices is observed. Therefore, it is more likely that both L^H_{M1} and L^H_{M2} are positive which implies unmixing tendencies in each of the two sublattices and hence ordering between them. Then, since$(L^H_{M1} - L^H_{M2}) > 0$, the unmixing tendencies must be stronger in the M1 than the M2 sublattice which conforms with the observation that in the octahedral chains, extending along [001], the M1-M1 distances are shorter than the M2-M2 distances, thus promoting larger interactions between the M1 than the M2 cations. To be more specific, in Mg-rich olivines, according to the larger value of L^H_{M1}, the fewer Fe^{2+} cations are more strongly driven from the M1 into the M2 sublattice than *vice versa* so that in total the crystal orders. On the other hand, in Fe^{2+}-rich crystals, the fewer Mg cations are forced to segregate from M1 into M2 which results in anti-order. It is thus the shorter <M1-M1> distance that accounts for the observed compositional variation of the exchange enthalpy. Kroll *et al*. (1997) found similar trends in orthopyroxenes where d(M2-M2) – d(M1-M1) ≈ 1.5 Å is even larger than in olivine with Δd ≈ 1 Å.

(4) Different from its enthalpic equivalent, $(L^S_{M1} - L^S_{M2})$ is a negative quantity, while ΔS^0_{exch} is positive. Therefore, in contrast to $\Delta H^0_{exch}(X)$,

Table 4a. Atomic fractional coordinates and anisotropic thermal displacement parameters [Å^2] of Acapulco olivine Aca-7 (Fa12.4), obtained from refinements with *ex situ* data (MS-data).

sample T [°C]		Aca-7 as is	Aca-7 500	Aca-7 550	Aca-7 600	Aca-7 650	Aca-7 700	Aca-7 750
Si	x	0.42683 (4)	0.42684 (4)	0.42681 (3)	0.42681 (4)	0.42684 (5)	0.42687 (4)	0.42687 (5)
	y	0.09440 (2)	0.09444 (2)	0.09445 (2)	0.09441 (2)	0.09443 (2)	0.09443 (2)	0.09445 (2)
	U_{11}	0.00337 (6)	0.00254 (6)	0.00291 (5)	0.00284 (6)	0.00273 (7)	0.00287 (7)	0.00287 (7)
	U_{22}	0.00409 (6)	0.00436 (6)	0.00423 (5)	0.00409 (6)	0.00396 (8)	0.00416 (7)	0.00439 (7)
	U_{33}	0.00417 (6)	0.00427 (6)	0.00414 (5)	0.00444 (6)	0.00452 (8)	0.00413 (7)	0.00451 (7)
	U_{12}	0.00014 (5)	0.00012 (5)	0.00012 (4)	0.00004 (5)	0.00019 (6)	0.00018 (6)	0.00018 (6)
M1	X_{Fe}	0.1166 (10)	0.1198 (9)	0.1203 (6)	0.1210 (8)	0.1214 (10)	0.1219 (8)	0.1235 (9)
	U_{11}	0.00526 (8)	0.00438 (8)	0.00478 (6)	0.00460 (7)	0.00458 (9)	0.00453 (8)	0.00489 (8)
	U_{22}	0.00712 (8)	0.00729 (8)	0.00722 (6)	0.00722 (8)	0.00694 (9)	0.00711 (8)	0.00737 (9)
	U_{33}	0.00484 (8)	0.00504 (8)	0.00495 (5)	0.00522 (7)	0.00517 (9)	0.00492 (8)	0.00514 (8)
	U_{12}	–0.00011 (6)	–0.00013 (6)	–0.00010 (5)	–0.00016 (6)	–0.00014 (7)	–0.00014 (7)	0.00001 (7)
	U_{13}	–0.00064 (6)	–0.00065 (6)	–0.00067 (5)	–0.00071 (6)	–0.00063 (8)	–0.00047 (7)	–0.00060 (7)
	U_{23}	–0.00112 (6)	–0.00116 (6)	–0.00116 (4)	–0.00124 (6)	–0.00119 (7)	–0.00110 (6)	–0.00106 (7)
M2	X_{Fe}	0.1134 (10)	0.1102 (9)	0.1097 (6)	0.1090 (8)	0.1086 (10)	0.1081 (8)	0.1065 (9)
	x	0.98951 (5)	0.98963 (5)	0.98961 (4)	0.98956 (5)	0.98966 (6)	0.98971 (5)	0.98971 (6)
	y	0.27775 (2)	0.27776 (2)	0.27775 (2)	0.27781 (2)	0.27773 (3)	0.27773 (2)	0.27778 (2)
	U_{11}	0.00665 (8)	0.00582 (9)	0.00622 (6)	0.00624 (8)	0.00614 (10)	0.00611 (9)	0.00620 (9)
	U_{22}	0.00467 (8)	0.00501 (8)	0.00485 (6)	0.00474 (7)	0.00467 (9)	0.00488 (8)	0.00494 (9)
	U_{33}	0.00553 (8)	0.00596 (8)	0.00571 (6)	0.00609 (7)	0.00593 (9)	0.00572 (8)	0.00614 (9)
	U_{12}	0.00014 (6)	0.00016 (7)	0.00017 (5)	0.00013 (6)	0.00028 (8)	0.00012 (7)	0.00026 (7)
O1	x	0.76587 (10)	0.76587 (11)	0.76582 (8)	0.76588 (10)	0.76600 (13)	0.76595 (11)	0.76593 (11)
	y	0.09157 (5)	0.09162 (5)	0.09164 (4)	0.09173 (5)	0.09166 (6)	0.09171 (5)	0.09178 (6)
	U_{11}	0.00337 (14)	0.00297 (14)	0.00313 (10)	0.00310 (13)	0.00313 (16)	0.00300 (15)	0.00284 (16)
	U_{22}	0.00714 (16)	0.00690 (16)	0.00726 (12)	0.00682 (15)	0.00710 (20)	0.00685 (17)	0.00696 (18)
	U_{33}	0.00524 (15)	0.00594 (15)	0.00561 (11)	0.00588 (14)	0.00585 (18)	0.00561 (15)	0.00604 (17)
	U_{12}	0.00031 (13)	0.00009 (14)	0.00012 (10)	0.00021 (13)	0.00023 (16)	0.00021 (14)	0.00013 (15)
O2	x	0.22022 (11)	0.22042 (12)	0.22026 (8)	0.22015 (11)	0.22011 (14)	0.22011 (12)	0.22003 (13)
	y	0.44784 (5)	0.44778 (5)	0.44781 (4)	0.44776 (5)	0.44776 (6)	0.44780 (5)	0.44780 (5)
	U_{11}	0.00554 (15)	0.00498 (16)	0.00520 (11)	0.00528 (15)	0.00514 (18)	0.00544 (17)	0.00528 (18)
	U_{22}	0.00407 (14)	0.00451 (15)	0.00420 (11)	0.00412 (14)	0.00435 (17)	0.00404 (15)	0.00452 (17)
	U_{33}	0.00621 (16)	0.00615 (16)	0.00608 (11)	0.00633 (15)	0.00614 (18)	0.00602 (16)	0.00628 (17)
	U_{12}	–0.00009 (13)	0.00016 (13)	0.00009 (10)	0.00002 (13)	–0.00005 (16)	–0.00010 (14)	0.00001 (15)
O3	x	0.27846 (7)	0.27866 (8)	0.27855 (6)	0.27871 (7)	0.27865 (9)	0.27878 (8)	0.27865 (8)
	y	0.16334 (3)	0.16335 (3)	0.16340 (2)	0.16339 (3)	0.16341 (4)	0.16339 (3)	0.16339 (4)
	z	0.03355 (6)	0.03354 (6)	0.03344 (4)	0.03339 (6)	0.03359 (7)	0.03357 (6)	0.03346 (7)
	U_{11}	0.00541 (10)	0.00476 (10)	0.00517 (7)	0.00514 (10)	0.00497 (12)	0.00502 (11)	0.00502 (11)
	U_{22}	0.00653 (10)	0.00671 (11)	0.00668 (8)	0.00668 (10)	0.00666 (13)	0.00655 (11)	0.00668 (12)
	U_{33}	0.00538 (10)	0.00541 (10)	0.00519 (8)	0.00549 (10)	0.00550 (12)	0.00534 (11)	0.00575 (12)
	U_{12}	0.00027 (9)	0.00033 (10)	0.00030 (7)	0.00035 (9)	0.00026 (12)	0.00020 (10)	0.00023 (11)
	U_{13}	–0.00016 (9)	–0.00024 (9)	–0.00024 (7)	–0.00012 (9)	–0.00019 (11)	–0.00025 (10)	–0.00028 (11)
	U_{23}	0.00160 (9)	0.00156 (9)	0.00168 (7)	0.00166 (9)	0.00152 (11)	0.00165 (10)	0.00165 (10)

Note: Special positions not listed above: x(M1) = y(M1) = z(M1) = 0, z(Si) = z(M2) = z(O1) = z(O2) = ¼.

$$\Delta S^0_{exch}(X) = \Delta S^0_{exch}(X = 0) - (L^S_{M1} - L^S_{M2})X \quad (12)$$

is predicted to decrease for compositions approaching the Mg endmember, and *vice versa* to increase towards the Fe endmember. Kroll *et al*. (2006) have considered ΔS^0_{exch} as a sum of two components, *viz*. a dominating exchange *vibrational* entropy and a much smaller exchange *electronic* entropy (about 0.3 J/molK for Fa50), the latter resulting from the distribution of the sixth d-electron of Fe^{2+} over the three t_{2g} electron levels. Then, starting from Fa50 and moving towards Fa0 the exchange electronic entropy decreases to zero since Mg has no d-electrons. Likewise, it increases to 0.6 J/molK in Fa100 where the Fe content is twice as large as in Fa50. The change of the electronic entropy may thus well contribute to the compositional variation of the exchange entropy.

Quenching experiments and resetting effects

The site occupancies of the olivine crystals Fa11.6 and Fa27.8 were obtained from *ex situ* experiments. Between 500 °C and 750 °C, no resetting effect disturbs the regular increases of $\ln K_D$ vs. 1/T (Fig. 2). On the other hand, the two samples, Fa27.6 and Fa27.8, quenched from 900 °C clearly show a Fe^{2+},Mg redistribution during quench. Their actual site occupancies correspond to apparent equilibrium temperatures, T_{ae}, of 760(33) °C and 806(37) °C, respectively,

Table 4b. Atomic fractional coordinates and anisotropic thermal displacement parameters [Å^2] of Acapulco olivine Aca-8 (Fa12.4), obtained from refinements with *ex situ* data (MS-data).

sample T [°C]		Aca-8 as is	Aca-8 500	Aca-8 550	Aca-8 600	Aca-8 650	Aca-8 700	Aca-8 750
Si	x	0.42680 (4)	0.42685 (3)	0.42682 (3)	0.42690 (4)	0.42683 (5)	0.42686 (4)	0.42688 (4)
	y	0.09440 (2)	0.09444 (2)	0.09447 (1)	0.09444 (2)	0.09447 (2)	0.09447 (2)	0.09445 (2)
	U_{11}	0.00318 (6)	0.00314 (5)	0.00286 (4)	0.00343 (6)	0.00335 (7)	0.00296 (6)	0.00292 (6)
	U_{22}	0.00411 (6)	0.00413 (5)	0.00406 (4)	0.00418 (6)	0.00427 (7)	0.00405 (6)	0.00418 (6)
	U_{33}	0.00429 (6)	0.00417 (5)	0.00423 (4)	0.00432 (6)	0.00404 (7)	0.00426 (6)	0.00431 (7)
	U_{12}	0.00013 (5)	0.00009 (4)	0.00007 (4)	0.00012 (5)	0.00021 (6)	0.00011 (5)	0.00014 (5)
M1	X_{Fe}	0.1155 (8)	0.1198 (7)	0.1200 (6)	0.1212 (9)	0.1215 (9)	0.1223 (8)	0.1237 (8)
	U_{11}	0.00506 (7)	0.00485 (6)	0.00462 (5)	0.00515 (7)	0.00497 (8)	0.00473 (7)	0.00479 (7)
	U_{22}	0.00693 (7)	0.00703 (7)	0.00700 (6)	0.00706 (8)	0.00707 (8)	0.00691 (8)	0.00711 (8)
	U_{33}	0.00503 (7)	0.00494 (6)	0.00495 (5)	0.00507 (7)	0.00483 (8)	0.00488 (7)	0.00501 (8)
	U_{12}	–0.00014 (6)	–0.00007 (5)	–0.00012 (4)	–0.00008 (6)	–0.00008 (6)	–0.00018 (6)	–0.00009 (6)
	U_{13}	–0.00067 (6)	–0.00064 (5)	–0.00063 (4)	–0.00065 (6)	–0.00058 (7)	–0.00058 (6)	–0.00067 (6)
	U_{23}	–0.00118 (6)	–0.00120 (5)	–0.00118 (4)	–0.00113 (6)	–0.00120 (6)	–0.00112 (6)	–0.00116 (6)
M2	X_{Fe}	0.1146 (8)	0.1102 (7)	0.1100 (6)	0.1088 (9)	0.1085 (9)	0.1077 (8)	0.1063 (8)
	x	0.98952 (5)	0.98959 (4)	0.98954 (4)	0.98960 (5)	0.98969 (5)	0.98958 (5)	0.98971 (5)
	y	0.27778 (2)	0.27778 (2)	0.27776 (2)	0.27777 (2)	0.27774 (2)	0.27774 (2)	0.27775 (2)
	U_{11}	0.00641 (8)	0.00638 (7)	0.00622 (6)	0.00656 (8)	0.00656 (9)	0.00624 (8)	0.00627 (8)
	U_{22}	0.00464 (7)	0.00468 (6)	0.00464 (6)	0.00481 (7)	0.00479 (8)	0.00464 (7)	0.00484 (8)
	U_{33}	0.00568 (7)	0.00577 (6)	0.00572 (5)	0.00589 (8)	0.00569 (8)	0.00576 (7)	0.00568 (8)
	U_{12}	0.00014 (6)	0.00017 (5)	0.00021 (4)	0.00015 (6)	0.00012 (7)	0.00017 (6)	0.00023 (6)
O1	x	0.76610 (9)	0.76593 (8)	0.76592 (7)	0.76604 (10)	0.76593 (11)	0.76590 (10)	0.76597 (10)
	y	0.09166 (5)	0.09169 (4)	0.09170 (4)	0.09167 (5)	0.09175 (5)	0.09160 (5)	0.09170 (5)
	U_{11}	0.00309 (13)	0.00327 (11)	0.00313 (10)	0.00356 (13)	0.00360 (15)	0.00328 (14)	0.00320 (14)
	U_{22}	0.00713 (15)	0.00694 (13)	0.00716 (12)	0.00717 (16)	0.00691 (17)	0.00682 (15)	0.00721 (16)
	U_{33}	0.00594 (14)	0.00571 (12)	0.00566 (10)	0.00573 (15)	0.00567 (16)	0.00581 (14)	0.00560 (15)
	U_{12}	0.00033 (12)	0.00024 (10)	0.00024 (9)	0.00031 (13)	0.00014 (14)	0.00046 (13)	0.00029 (13)
O2	x	0.22033 (10)	0.22014 (9)	0.22017 (8)	0.21998 (11)	0.22004 (12)	0.22003 (11)	0.22021 (11)
	y	0.44777 (4)	0.44779 (4)	0.44774 (3)	0.44780 (5)	0.44785 (5)	0.44781 (5)	0.44783 (5)
	U_{11}	0.00534 (14)	0.00531 (12)	0.00523 (11)	0.00554 (15)	0.00558 (16)	0.00540 (15)	0.00537 (15)
	U_{22}	0.00416 (13)	0.00413 (12)	0.00428 (10)	0.00436 (14)	0.00417 (15)	0.00405 (14)	0.00406 (15)
	U_{33}	0.00610 (14)	0.00618 (13)	0.00615 (11)	0.00627 (15)	0.00590 (16)	0.00635 (15)	0.00620 (16)
	U_{12}	–0.00016 (12)	–0.00012 (10)	–0.00002 (9)	–0.00003 (12)	–0.00023 (14)	–0.00006 (12)	–0.00032 (13)
O3	x	0.27867 (7)	0.27871 (6)	0.27854 (5)	0.27871 (7)	0.27872 (8)	0.27882 (7)	0.27863 (7)
	y	0.16334 (3)	0.16342 (3)	0.16340 (2)	0.16337 (3)	0.16336 (4)	0.16342 (3)	0.16337 (3)
	z	0.03343 (6)	0.03346 (5)	0.03343 (4)	0.03351 (6)	0.03347 (6)	0.03352 (6)	0.03354 (6)
	U_{11}	0.00542 (9)	0.00547 (8)	0.00516 (7)	0.00553 (10)	0.00552 (11)	0.00527 (10)	0.00519 (10)
	U_{22}	0.00658 (10)	0.00650 (8)	0.00654 (8)	0.00658 (10)	0.00652 (11)	0.00651 (10)	0.00658 (11)
	U_{33}	0.00541 (10)	0.00555 (8)	0.00530 (7)	0.00561 (10)	0.00539 (11)	0.00537 (10)	0.00540 (11)
	U_{12}	0.00030 (9)	0.00036 (8)	0.00028 (7)	0.00031 (9)	0.00022 (10)	0.00017 (9)	0.00027 (9)
	U_{13}	–0.00026 (9)	–0.00016 (7)	–0.00021 (6)	–0.00023 (9)	–0.00007 (10)	–0.00015 (9)	–0.00027 (9)
	U_{23}	0.00163 (9)	0.00172 (7)	0.00157 (6)	0.00154 (9)	0.00169 (10)	0.00161 (9)	0.00166 (9)

Note: Special positions not listed above: x(M1) = y(M1) = z(M1) = 0, z(Si) = z(M2) = z(O1) = z(O2) = ¼.

T_{ae} being obtained from equation (9). These findings confirm the results of Morozov *et al*. (2001, 2002, 2005) and Heinemann *et al*. (2006) who concluded that olivines should be quenchable from at least 750 °C without noticeable resetting effects. These results are in contrast to Redfern *et al*. (2000).

State of order and cooling history

Redfern *et al*. (2000) introduced the so-called crossover temperature T_{co}. Upon cooling a crystal passes at this temperature the border between the regimes of anti-order (Q < 0) and order (Q > 0). At T_{co} the crystal is fully disordered, *i.e.* – $RT_{co}\ \ln K_D = \Delta H^0_{exch}(X) - T_{co}\ \Delta S^0_{exch}(X) = 0$.

Since, as seen, $\Delta H^0_{exch}(X)$ decreases towards the Fe endmember whereas $\Delta S^0_{exch}(X)$ increases, T_{co} also decreases in that direction (Fig. 3), and since T_{co} is generally low, only slowly cooled Mg-rich olivines can be expected in the regime of ordered Fe^{2+},Mg distributions. In slowly cooled orthopyroxenes, the Fe^{2+},Mg exchange process effectively freezes in at an apparent equilibrium temperature T_{ae} as low as 300 °C – 200 °C (Tribaudino and Talarico, 1992; Ganguly *et al.*, 1994; Stimpfl *et al*., 2005). T_{ae} in olivines can be expected similarly low. Assuming the lowest attainable T_{ae} somewhere between 250 °C and 200 °C, only olivines with

Table 4c. Atomic fractional coordinates and anisotropic thermal displacement parameters [Å^2] of South Madagascar [Ro 8/2 (Fa12.4)] and Saar-Nahe [CSR-1 (Fa27.8), CSR-5 (Fa25.6), CSR-12 (Fa27.6)] olivines, obtained from refinements with *ex situ* data (MS-data).

sample		Ro 8/2	CSR-1	CSR-1	CSR-1	CSR-1	CSR-1	CSR-5	CSR-12	CSR-12	CSR-12	CSR-12
T [°C]		as is	as is	550	625	700	900	as is	550	625	700	900
Si	x	0.42671 (2)	0.42752 (4)	0.42748 (3)	0.42751 (3)	0.42748 (3)	0.42753 (3)	0.42737 (3)	0.42749 (3)	0.42750 (3)	0.42749 (3)	0.42747 (3)
	y	0.09434 (1)	0.09508 (2)	0.09505 (1)	0.09509 (1)	0.09511 (2)	0.09511 (1)	0.09499 (1)	0.09503 (2)	0.09509 (1)	0.09509 (2)	0.09509 (2)
	U_{11}	0.00320 (3)	0.00392 (6)	0.00434 (4)	0.00402 (4)	0.00448 (5)	0.00417 (5)	0.00344 (4)	0.00356 (5)	0.00370 (4)	0.00363 (5)	0.00395 (5)
	U_{22}	0.00467 (3)	0.00485 (6)	0.00512 (4)	0.00497 (4)	0.00506 (5)	0.00518 (4)	0.00489 (4)	0.00526 (5)	0.00487 (5)	0.00543 (5)	0.00514 (5)
	U_{33}	0.00462 (3)	0.00506 (6)	0.00520 (4)	0.00494 (4)	0.00498 (5)	0.00515 (4)	0.00495 (4)	0.00537 (5)	0.00467 (4)	0.00510 (5)	0.00530 (5)
	U_{12}	0.00015 (2)	0.00024 (5)	0.00020 (4)	0.00024 (3)	0.00025 (4)	0.00026 (4)	0.00023 (3)	0.00020 (4)	0.00022 (4)	0.00023 (4)	0.00020 (4)
M1	X_{Fe}	0.1197 (4)	0.2945 (7)	0.2947 (6)	0.2972 (6)	0.2985 (7)	0.2998 (6)	0.2703 (5)	0.2929 (6)	0.2948 (6)	0.2966 (6)	0.2986 (6)
	U_{11}	0.00475 (3)	0.00524 (6)	0.00563 (4)	0.00527 (4)	0.00572 (5)	0.00545 (4)	0.00482 (4)	0.00494 (4)	0.00478 (4)	0.00484 (5)	0.00506 (4)
	U_{22}	0.00739 (4)	0.00729 (6)	0.00772 (4)	0.00750 (4)	0.00749 (5)	0.00766 (4)	0.00755 (4)	0.00778 (5)	0.00738 (4)	0.00790 (5)	0.00762 (5)
	U_{33}	0.00505 (4)	0.00525 (5)	0.00558 (4)	0.00516 (4)	0.00522 (5)	0.00538 (4)	0.00526 (4)	0.00565 (5)	0.00498 (4)	0.00543 (5)	0.00558 (4)
	U_{12}	–0.00014 (2)	–0.00004 (4)	–0.00009 (3)	–0.00005 (3)	–0.00003 (4)	–0.00006 (3)	–0.00006 (3)	0.00000 (4)	–0.00008 (3)	–0.00002 (4)	–0.00004 (4)
	U_{13}	–0.00065 (3)	–0.00061 (4)	–0.00064 (3)	–0.00062 (3)	–0.00066 (4)	–0.00065 (3)	–0.00060 (3)	–0.00064 (4)	–0.00062 (3)	–0.00057 (4)	–0.00064 (4)
	U_{23}	–0.00114 (3)	–0.00123 (4)	–0.00127 (3)	–0.00129 (3)	–0.00128 (4)	–0.00129 (3)	–0.00124 (3)	–0.00128 (4)	–0.00127 (3)	–0.00131 (4)	–0.00124 (4)
M2	X_{Fe}	0.1239 (4)	0.2573 (7)	0.2571 (6)	0.2546 (6)	0.2533 (7)	0.2520 (6)	0.2389 (5)	0.2553 (6)	0.2534 (6)	0.2516 (6)	0.2496 (6)
	x	0.98905 (2)	0.98772 (4)	0.98782 (3)	0.98772 (3)	0.98780 (3)	0.98787 (3)	0.98788 (3)	0.98786 (3)	0.98778 (3)	0.98786 (3)	0.98785 (3)
	y	0.27787 (1)	0.27829 (2)	0.27822 (1)	0.27825 (1)	0.27827 (1)	0.27825 (1)	0.27818 (1)	0.27826 (1)	0.27824 (1)	0.27825 (1)	0.27824 (1)
	U_{11}	0.00631 (4)	0.00691 (6)	0.00749 (5)	0.00713 (4)	0.00758 (6)	0.00730 (5)	0.00664 (4)	0.00679 (5)	0.00674 (5)	0.00668 (6)	0.00694 (5)
	U_{22}	0.00495 (3)	0.00467 (6)	0.00509 (4)	0.00483 (4)	0.00489 (5)	0.00503 (4)	0.00487 (4)	0.00520 (5)	0.00468 (4)	0.00529 (5)	0.00500 (5)
	U_{33}	0.00586 (3)	0.00566 (6)	0.00600 (4)	0.00562 (4)	0.00564 (5)	0.00583 (4)	0.00579 (4)	0.00612 (5)	0.00545 (4)	0.00578 (5)	0.00599 (5)
	U_{12}	0.00017 (2)	0.00018 (5)	0.00014 (3)	0.00013 (3)	0.00014 (4)	0.00012 (4)	0.00014 (3)	0.00016 (4)	0.00010 (4)	0.00019 (4)	0.00011 (4)
O1	x	0.76570 (5)	0.76614 (10)	0.76606 (7)	0.76608 (7)	0.76599 (9)	0.76619 (7)	0.76599 (6)	0.76599 (8)	0.76600 (7)	0.76603 (8)	0.76600 (8)
	y	0.09143 (2)	0.09182 (5)	0.09193 (4)	0.09194 (3)	0.09193 (4)	0.09199 (4)	0.09185 (3)	0.09192 (4)	0.09195 (4)	0.09192 (4)	0.09198 (4)
	U_{11}	0.00337 (6)	0.00399 (14)	0.00447 (10)	0.00428 (9)	0.00463 (12)	0.00455 (11)	0.00353 (8)	0.00384 (11)	0.00382 (10)	0.00391 (12)	0.00412 (11)
	U_{22}	0.00763 (7)	0.00838 (16)	0.00863 (11)	0.00841 (10)	0.00859 (13)	0.00848 (12)	0.00840 (10)	0.00862 (13)	0.00819 (12)	0.00883 (14)	0.00852 (13)
	U_{33}	0.00594 (7)	0.00637 (14)	0.00665 (10)	0.00629 (9)	0.00647 (12)	0.00648 (11)	0.00639 (9)	0.00674 (12)	0.00625 (11)	0.00652 (12)	0.00671 (12)
	U_{12}	0.00028 (5)	0.00021 (13)	0.00041 (9)	0.00022 (8)	0.00026 (10)	0.00021 (10)	0.00028 (7)	0.00034 (10)	0.00022 (9)	0.00023 (11)	0.00029 (10)
O2	x	0.22060 (5)	0.21788 (11)	0.21784 (8)	0.21766 (7)	0.21772 (9)	0.21769 (8)	0.21823 (7)	0.21798 (9)	0.21784 (8)	0.21763 (9)	0.21770 (9)
	y	0.44788 (2)	0.44892 (4)	0.44884 (3)	0.44891 (3)	0.44896 (4)	0.44889 (3)	0.44873 (3)	0.44892 (4)	0.44890 (3)	0.44884 (4)	0.44896 (4)
	U_{11}	0.00560 (7)	0.00665 (15)	0.00711 (11)	0.00691 (10)	0.00737 (13)	0.00696 (11)	0.00631 (9)	0.00634 (12)	0.00643 (11)	0.00652 (13)	0.00656 (12)
	U_{22}	0.00438 (6)	0.00492 (14)	0.00516 (10)	0.00495 (9)	0.00496 (12)	0.00511 (10)	0.00466 (8)	0.00530 (12)	0.00485 (10)	0.00529 (12)	0.00488 (11)
	U_{33}	0.00650 (7)	0.00695 (15)	0.00719 (11)	0.00703 (10)	0.00703 (12)	0.00705 (11)	0.00694 (9)	0.00741 (13)	0.00682 (11)	0.00702 (13)	0.00738 (13)
	U_{12}	–0.00005 (5)	0.00000 (13)	–0.00002 (9)	–0.00017 (8)	–0.00012 (10)	0.00003 (9)	–0.00009 (7)	0.00000 (10)	–0.00001 (9)	–0.00005 (11)	0.00002 (10)
O3	x	0.27871 (3)	0.28054 (7)	0.28042 (5)	0.28050 (5)	0.28061 (6)	0.28065 (5)	0.28017 (5)	0.28045 (6)	0.28052 (5)	0.28056 (6)	0.28051 (6)
	y	0.16317 (2)	0.16384 (3)	0.16380 (2)	0.16382 (2)	0.16381 (3)	0.16383 (2)	0.16370 (2)	0.16376 (3)	0.16380 (2)	0.16377 (3)	0.16383 (3)
	z	0.03366 (3)	0.03411 (6)	0.03411 (4)	0.03410 (4)	0.03416 (5)	0.03411 (4)	0.03409 (4)	0.03411 (5)	0.03407 (4)	0.03413 (5)	0.03407 (5)
	U_{11}	0.00546 (4)	0.00662 (10)	0.00676 (7)	0.00658 (7)	0.00694 (9)	0.00663 (8)	0.00597 (6)	0.00624 (8)	0.00604 (7)	0.00622 (8)	0.00623 (8)
	U_{22}	0.00708 (5)	0.00754 (10)	0.00799 (7)	0.00780 (7)	0.00789 (9)	0.00795 (8)	0.00770 (6)	0.00787 (9)	0.00773 (8)	0.00806 (9)	0.00793 (8)
	U_{33}	0.00575 (5)	0.00647 (10)	0.00661 (7)	0.00639 (6)	0.00641 (8)	0.00655 (7)	0.00632 (6)	0.00674 (9)	0.00611 (7)	0.00654 (9)	0.00669 (8)
	U_{12}	0.00027 (4)	0.00055 (9)	0.00041 (7)	0.00037 (6)	0.00039 (8)	0.00041 (7)	0.00038 (5)	0.00045 (8)	0.00040 (7)	0.00040 (8)	0.00048 (7)
	U_{13}	–0.00030 (4)	–0.00024 (9)	–0.00030 (6)	–0.00034 (6)	–0.00032 (7)	–0.00035 (6)	–0.00029 (5)	–0.00028 (7)	–0.00020 (6)	–0.00035 (8)	–0.00024 (7)
	U_{23}	0.00178 (4)	0.00200 (9)	0.00207 (6)	0.00207 (6)	0.00216 (7)	0.00205 (7)	0.00207 (5)	0.00210 (8)	0.00201 (7)	0.00199 (8)	0.00215 (7)

Note: Special positions not listed above: x(M1) = y(M1) = z(M1) = 0, z(Si) = z(M2) = z(O1) = z(O2) = ¼.

compositions <Fa25 are able to enter the regime of order because only there $T_{co} > T_{ae}$.

The olivine Ro8/2 (Fa12.4) from a granulite-facies marble from South Madagascar (Table 5) is an example for such a case. Its $\ln K_D$ value corresponds to $T_{ae} = 224(8)$ °C (Fig. 2) while $\ln K_D = 0$ is obtained at $T_{co} = 340$°C, *i.e.* $T_{co} > T_{ae}$.

The slow cooling of the host rock may be confirmed by a cooling rate calculation applying the rate equation of Mueller (1967, 1969) which has been exemplified, among others, by Ganguly (1982) and Kroll *et al.* (1997). Other suitable rate laws suggested in the literature have been compared and evaluated by Kroll (2003). For our calculation, the $\ln K_D$ line for Fa12.4 was taken from equations (9) and (10), and the temperature variation of the rate constant for the Fe^{2+},Mg exchange process was obtained following the procedure outlined by Heinemann *et al.* (1999, 2006). The resulting cooling rate is –1 °C/My with an error of a factor of 3 that is due to the standard deviation in X_{Fe}^{M2}. The result appears to be quite a reasonable order-of-magnitude estimate for the low temperature cooling of a metamorphic rock.

The ordering history of the Ro8/2 olivine is thus as follows (Fig. 2, Fig. 4). At some high temperature, the crystal was anti-ordered, $Q < 0$. First, during cooling, Fe^{2+} fractionated into M2 which led to increasing disorder. Then, $Q = 0$ was attained at 340 °C, and from thereon further segregation of Fe^{2+} into M2 lead to increasing order, $Q > 0$. This process ended at a temperature near $T_{ae} = 224$ °C.

Contrasting to the granulite-facies olivine, the two olivines Fa25.6 and Fa27.8 from the lava flow (Table 5, CSR-5 and CSR-1, "as is") feature higher Fa contents and higher apparent equilibrium temperatures, $T_{ae} = 511(23)$ °C and $T_{ae} = 528(24)$ °C, respectively. Both have been captured in anti-ordered states (Fig. 2, 4). Their cooling rate estimates of –11 °C/d and –28 °C/d (each with an error of a factor of 3) qualify also as reasonable order-of-magnitude estimates.

Table 5. Agreement factors (%), site occupancies and distribution coefficients.

data set				T (°C)	R_w	R_u	GoF	X_{Fe}^{M2}	$\sigma(X_{Fe}^{M2})$	X_{Mg}^{M2}	X_{Fe}^{M1}	X_{Mg}^{M1}	$\overline{X}_{Fe}^{M2}$	$\overline{X}_{Fe}^{M1}$	K_D	$\ln K_D$	$\sigma(\ln K_D)$
MS	Fa 12.4	Ro	–8/2	as is	1.09	1.16	1.07	0.1239	0.0004	0.8360	0.1197	0.8803	0.1291	0.1197	0.917	–0.087	0.007
MS	Fa 11.6	Aca	–7–1	as is	1.75	1.85	0.70	0.1134	0.0010	0.8766	0.1166	0.8834	0.1146	0.1166	1.020	0.020	0.020
			–7–2	500	1.71	1.88	0.61	0.1102	0.0009	0.8798	0.1198	0.8802	0.1113	0.1198	1.087	0.083	0.017
			–7–3	550	1.26	1.53	0.63	0.1097	0.0006	0.8803	0.1203	0.8797	0.1108	0.1203	1.097	0.093	0.013
			–7–4	600	1.57	1.74	0.56	0.1091	0.0008	0.8810	0.1210	0.8791	0.1102	0.1210	1.112	0.106	0.016
			–7–5	650	2.07	2.17	0.68	0.1086	0.0010	0.8814	0.1214	0.8786	0.1097	0.1214	1.121	0.114	0.021
			–7–6	700	1.62	1.88	0.58	0.1081	0.0008	0.8819	0.1219	0.8781	0.1092	0.1219	1.132	0.124	0.016
			–7–7	750	1.74	2.15	0.79	0.1065	0.0009	0.8835	0.1235	0.8765	0.1076	0.1235	1.169	0.156	0.018
		Aca	–8–1	as is	1.56	1.90	0.86	0.1146	0.0008	0.8755	0.1155	0.8846	0.1157	0.1155	0.998	–0.003	0.015
			–8–2	500	1.45	1.57	0.60	0.1102	0.0007	0.8798	0.1198	0.8802	0.1113	0.1198	1.086	0.083	0.014
			–8–3	550	1.29	1.46	0.63	0.1100	0.0006	0.8800	0.1200	0.8800	0.1111	0.1200	1.091	0.087	0.012
			–8–4	600	1.72	1.87	0.69	0.1088	0.0009	0.8812	0.1212	0.8788	0.1099	0.1212	1.118	0.111	0.017
			–8–5	650	1.74	2.09	0.83	0.1085	0.0009	0.8815	0.1215	0.8785	0.1096	0.1215	1.124	0.117	0.017
			–8–6	700	1.57	1.74	0.62	0.1077	0.0008	0.8823	0.1223	0.8777	0.1088	0.1223	1.142	0.133	0.016
			–8–7	750	1.68	2.01	0.83	0.1063	0.0008	0.8837	0.1237	0.8763	0.1074	0.1237	1.173	0.160	0.016
BN	Fa 22.3	CSR	–2–1	20	1.48	1.36	1.29	0.2073	0.0008	0.7805	0.2364	0.7636	0.2099	0.2364	1.165	0.153	0.009
			–2–2	450	1.61	1.54	1.26	0.2072	0.0009	0.7806	0.2365	0.7635	0.2098	0.2365	1.167	0.154	0.010
			–2–3	600	1.51	1.47	1.14	0.2041	0.0008	0.7837	0.2396	0.7604	0.2066	0.2396	1.210	0.190	0.010
			–2–4	677	1.51	1.32	1.13	0.2042	0.0008	0.7836	0.2395	0.7605	0.2067	0.2395	1.209	0.190	0.010
			–2–5	725	1.44	1.35	1.08	0.2038	0.0008	0.7840	0.2399	0.7601	0.2063	0.2399	1.214	0.194	0.009
			–2–6	800	1.45	1.36	1.05	0.2021	0.0008	0.7857	0.2416	0.7584	0.2046	0.2416	1.238	0.214	0.009
MS	Fa 25.6	CSR	–5–1	as is	1.21	1.25	0.74	0.2389	0.0005	0.7477	0.2703	0.7297	0.2421	0.2703	1.159	0.148	0.006
MS	Fa 27.6	CSR	–12–1	550	1.34	1.47	0.65	0.2553	0.0006	0.7284	0.2929	0.7071	0.2595	0.2929	1.182	0.167	0.006
			–12–2	625	1.25	1.40	0.72	0.2534	0.0006	0.7303	0.2948	0.7052	0.2576	0.2948	1.205	0.187	0.006
			–12–3	700	1.31	1.50	0.69	0.2516	0.0006	0.7321	0.2966	0.7034	0.2557	0.2966	1.227	0.205	0.006
			–12–4	900	1.20	1.47	0.66	0.2495	0.0006	0.7341	0.2986	0.7014	0.2537	0.2986	1.252	0.225	0.006
MS	Fa 27.8	CSR	–1–1	as is	1.60	1.73	0.73	0.2573	0.0007	0.7265	0.2945	0.7055	0.2615	0.2945	1.179	0.165	0.007
			–1–2	550	1.16	1.35	0.72	0.2571	0.0006	0.7267	0.2947	0.7053	0.2613	0.2947	1.181	0.167	0.006
			–1–3	625	1.23	1.31	0.83	0.2546	0.0006	0.7292	0.2972	0.7028	0.2588	0.2972	1.211	0.191	0.006
			–1–4	700	1.57	1.62	1.03	0.2533	0.0007	0.7305	0.2985	0.7015	0.2575	0.2985	1.227	0.205	0.007
			–1–5	900	1.15	1.40	0.78	0.2520	0.0006	0.7318	0.2998	0.7002	0.2561	0.2998	1.244	0.218	0.006

$X_{Mg}^{M1} = 1 - X_{Fe}^{M1}$ $X_{Mg}^{M2} = 1 - X_{Ca}^{M2} - X_{Mn}^{M2} - X_{Fe}^{M2}$ $\overline{X}_{Fe}^{M2} = X_{Fe}^{M2}/(X_{Fe}^{M2} + X_{Mg}^{M2})$ $\overline{X}_{Fe}^{M1} = X_{Fe}^{M1}/(X_{Fe}^{M1} + X_{Mg}^{M1})$ $K_D = X_{Fe}^{M1} \times X_{Mg}^{M2}/X_{Fe}^{M2} \times X_{Mg}^{M1} = \overline{X}_{Fe}^{M1}(1 - \overline{X}_{Fe}^{M2})/\overline{X}_{Fe}^{M2}(1 - \overline{X}_{Fe}^{M1})$

$$R = \frac{\Sigma(|F_o - F_c|)}{\Sigma(F_o)} \quad R_W = \left(\frac{\Sigma w \times (F_o - F_c)^2}{\Sigma w \times F_o^2}\right)^{1/2} \quad GoF = \left(\frac{\Sigma w \times (F_o - F_c)^2}{(N_{hkl} - P)}\right)^{1/2} = \text{goodness of fit.}$$

N_{hkl} = number of reflections, P = number of independent parameters, $(N_{hkl} - P)$ = degrees of freedom

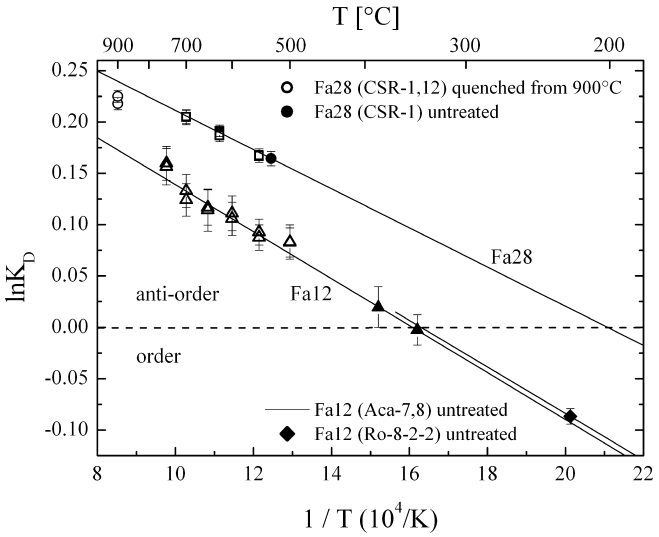

Fig. 2. Variation of $\ln K_D$ of the samples Fa11.6, Fa27.6 and Fa27.8 with inverse temperature as in Figure 1. Data of the metamorphic olivine Ro-8/2, of the untreated crystals Aca-7, 8 and CSR-1 and those of the quenched crystals CSR-1, 12 are added (Table 5). The data points of the untreated crystals represent two types of cooling: fast volcanic (Fa28) as opposed to slow metamorphic (Fa12.4). Evidently, Fe^{2+},Mg site distributions that are ordered can only be expected from slow cooling, fast cooling freezes at ordered distributions.

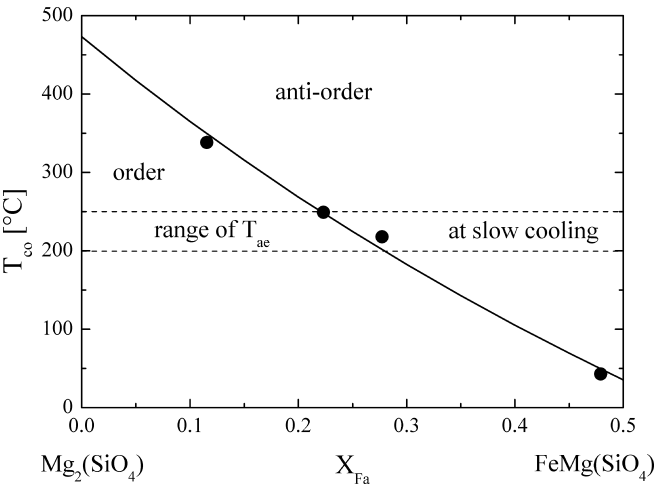

Fig. 3. Variation of the crossover temperature $T_{co} = \Delta H^0_{exch}(X) / \Delta S^0_{exch}(X)$ with composition $X = 2X_{Fa}-1$. At T_{co}, anti-ordering turns into ordering with decreasing temperature. The respective T_{co} values (full circles) were calculated from individual fits to the $\ln K_D$ lines in Fig. 1. The curvature of the lines derives from equations (11) and (12). For metamorphic cooling, the Fe^{2+},Mg site exchange processes may be effective down to 250 °C to 200 °C before freezing (horizontal T_{ae} range). Thus, ordered Fe^{2+},Mg site distributions can only be realized in Mg-rich olivines, for which $T_{ae}<T_{co}$.

In contrast to the metamorphic and volcanic olivines, the *a priori* unknown cooling history of the Acapulco meteorite precludes the comparison of our results with rates expected from geological reasoning. Using Fe^{2+},Mg geospeedometry on Acapulco orthopyroxene, Zema *et al*. (1996) estimated a rate of –60 °C/y at 490 °C, however, on the basis of a possibly inadequate calibration for $\ln K_D(T)$. Using the classical metallographic technique and the Ni concentration in taenite, McCoy *et al*. (1996) arrived at a rate of about –0.1 °C/y between 600°C and 400 °C. The minimum estimated cooling rate is –3.7 °C/My between 450 °C and 290 °C as obtained by Pellas *et al*. (1997) who applied radiogenic and fission track methods. Both our two untreated Acapulco crystals, Aca-7-as is and Aca-8-as is, show Fe^{2+},Mg distributions close to disorder and corresponding to apparent equilibrium temperatures of 385(37) °C and 344(26) °C, respectively (Fig. 2, 4). Thus, the Acapulco crystals must have cooled faster than the metamorphic olivine. The cooling rate calculation yielded –1 °C/y and –0.05 °C/y near the respective T_{ae}, each rate being associated with an uncertainty of about a factor of 10. In view of the large discrepancies produced by the various methods as discussed by Pellas *et al.* (1997) the rates obtained here can be considered close to those reported by Zema *et al.* (1996) and McCoy *et al.* (1996).

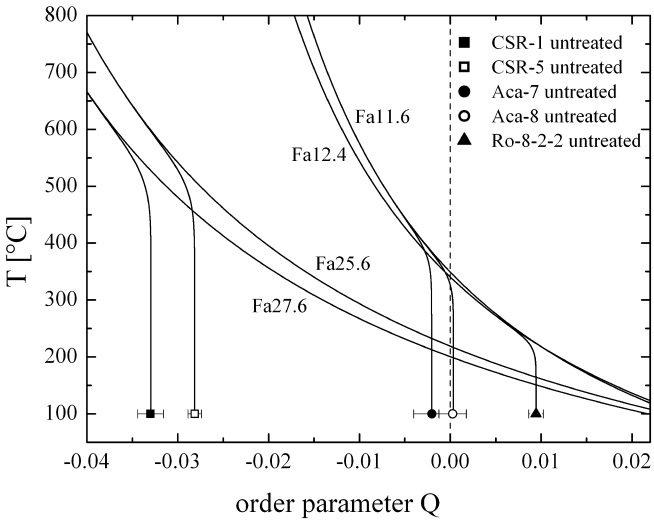

Fig. 4. Ordering path simulations of (a) the metamorphic olivine Ro8/2 (Fa12.4), (b) the volcanic olivines CRS-5 (Fa25.6) and CSR-1 (Fa27.8) and (c) the meteoric olivines Aca-7 and Aca-8 (Fa11.6). At elevated temperatures, the ordering paths follow the respective equilibrium curves from which the deviate at temperatures that increase with increasing cooling rates.

Conclusion

Heinemann *et al*. (2006) investigated the temperature dependence of the Fe^{2+},Mg site distribution in Fa47.8 and found in agreement with Morozov *et al*. (2005), but at variance with Redfern *et al*. (2000), that the Fe^{2+} concentration on the M1 site continuously increases with rising temperature so that anti-order increases. The present study extends the investigation to Mg-richer compositions. Assuming that the results of Artioli *et al*. (1995), Rinaldi *et al*. (2000) and Redfern *et al*. (2000) are correct, one would expect that the *in situ* measured olivines Fa22.3 and Fa47.9 exhibit the predicted reversal of order at high temperatures. This is not the case, and even more so, only the samples Fa27.6 and Fa27.8 quenched from the highest temperature (900 °C) display the expected resetting effects towards disorder.

Olivine Fa47.8 is characterized by a very small exchange enthalpy of only 1.16 kJ/mol leading to a very gentle slope

Table 6. Unit-cell dimensions [Å] and volumes [Å^3] of Saar-Nahe olivine CSR-2 (Fa22.3). Standard deviations given in parentheses refer to the last decimal place(s).

sample	T (°C)	a_0	b_0	c_0	V
CSR–2–1	20	4.7733 (7)	10.2676(10)	6.0112 (6)	294.61 (6)
–2–2	450	4.7908 (9)	10.3232(12)	6.0434 (6)	298.88 (7)
–2–3	600	4.7967(12)	10.3412(29)	6.0543 (8)	300.32(12)
–2–4	677	4.8010(21)	10.3537(18)	6.0613(14)	301.30(16)
–2–5	725	4.8046(11)	10.3634(16)	6.0668 (6)	302.08 (9)
–2–6	800	4.8081(23)	10.3727(20)	6.0722(15)	302.84(17)

of the $\ln K_D$ line and hence to Fe^{2+},Mg distributions that are close to disorder at all temperatures. Ghose (1982) already argued that the ordering tendency due to cation size effects is almost balanced by anti-ordering effects due to bonding requirements. Kroll *et al*. (2006) could shape the qualitative argument into a quantitative and predictive one. The present study shows that the exchange enthalpy increases somewhat towards the Mg endmember, while the exchange entropy decreases. Consequently, the crossover temperature $T_{co} = \Delta H^0_{exch}(X)/\Delta S^0_{exch}(X)$ at which during cooling anti-order turns into order rises from about 50 °C for Fa50 to about 450 °C for Fa5. As a result, only Mg-rich olivines can be expected to attain ordered Fe^{2+},Mg site distributions. Olivines with more than about 25 mol% Fa content remain anti-ordered even at slow cooling.

Although our cooling rate calculations produced reasonable answers, we do not consider these results fit to justify the establishment of olivine as a geospeedometer. In our case, several circumstances were apparently (and maybe fortuitously) fulfilled: (1) the site occupancies in the untreated crystals could be determined with sufficient accuracy, (2) the temperature dependences of the Fe^{2+},Mg site distributions could be correctly determined, (3) modelling their variation with temperature and composition according to Thompson (1969, 1970) was successful, and (4) the modelling of the temperature and composition dependence of the rate constant for the Fe^{2+},Mg site exchange according to Heinemann et al. (1999, 2006) seems essentially correct. Nevertheless, the possibility that errors and inaccuracies may have compensated each other cannot be fully discarded. Thus, the problems inherent in an olivine geospeedometer, particularly the very limited variation of $\ln K_D$ with temperature and composition, continue to be severe enough to make its *routine* application questionable.

Acknowledgement: This work was supported by grants given by the Deutsche Forschungsgemeinschaft to Herbert Kroll and Armin Kirfel which is gratefully acknowledged. Our thanks are also due to Dr. Cornelia Schmidt-Riegraf, Münster, and Prof. Michael Raith, Bonn, who kindly donated olivine samples CSR and Ro8/2, respectively, as well as to Dr. Michael Enders, Münster, who performed careful electron microprobe analyses. H. K. is especially grateful to Dr. Victor Vinograd, Frankfurt, for many enlightening and pleasant discussions.

References

Aikawa, N., Kumazawa, M., Tokonami, M. (1985): Temperature dependence of intersite distribution of Mg and Fe in Olivine and the associated change of lattice parameters. *Phys. Chem. Minerals*, **12**, 1–8.

Artioli, G., Rinaldi, R., Wilson, C., Zanazzi, P.F. (1995): High-temperature Fe-Mg cation partitioning in olivine: In-situ single-crystal neutron diffraction study. *Am. Mineral.*, **80**, 197–200.

Becker, P.J. & Coppens, P. (1974): Extinction within the limit of validity of the Darwin transfer equations. I. General formalism for primary and secondary extinction and their application to spherical crystals. *Acta Cryst.*, **A30**, 129–147.

Cromer, D.T. & Waber, J.T. (1974): Atomic scattering factors for X-rays. *in* "International tables for X-ray crystallography, Vol. IV." J.A. Ibers and W.A. Hamilton, eds., Kynoch, Birmingham.

Doyle, P.A. & Turner, P.S. (1968): Relativistic Hartree-Fock X-ray and electron scattering factors. *Acta Cryst.*, **A24**, 390–397.

Finger, L.W. & Prince, E. (1975): A system of FORTRAN IV computer programs for crystal structural computations. *NBS Tech. Note*, 854.

Freiheit V., Heinemann R., Kroll H., Krane H.-G., Kirfel A. (2000) Thermal history of natural olivines from the temperature dependent cation distribution determined by laboratory and synchroton radiation X-ray diffraction. HASYLAB Annual Report 2000.

Ganguly, J. (1982): Mg-Fe order-disorder in ferromagnesian silicates. II. Thermodynamics, kinetics, and geological implications. *in* "Advances in Physical Geochemistry", Vol. 2, S.K. Saxena, ed., Springer, New York, 58–99.

Ganguly, J., Yang, H., Ghose, S. (1994): Thermal history of mesosiderites: Quantitative constraints from compositional zoning and Fe-Mg ordering in orthopyroxenes. *Geochim. Cosmochim. Acta*, **58**, 2711–2723.

Ghose, S. (1982): Mg-Fe order-disorder in ferromagnesian silicates. I. Crystal Chemistry. *in* "Advances in Physical Geochemistry". S.K. Saxena, Ed., **2**, 4–57, Springer, New York.

Heinemann, R., Staack, V., Fischer, A., Kroll, H., Vad, Th., Kirfel, A. (1999): Temperature dependences of Fe,Mg partitioning in Acapulco olivine. *Am. Mineral.*, **84**, 1400–1405.

Heinemann, R., Kroll, H., Kirfel, A., Barbier, B. (2003a): Die kontroverse Diskussion des Ordnungsverhaltens von Fe^{2+} und Mg in Olivinen. *Mitt. Österr. Mineral. Ges.*, **148**, 159–160.

–,–,–,– (2003b): Die Temperaturabhängigkeit der Fe^{2+},Mg-Verteilung in Olivinen. *Beih. z. Eur. J. Mineral.*, **15**(1), 78.

–,–,–,– (2006): Order and anti-order in olivine I: Structural response to temperature. *Eur. J. Mineral.*, **18**, 673–689.

Hovestreydt, E. (1983): On the atomic scattering factor for O^{2-}. *Acta Cryst.*, **A39**, 268–269.

Kroll, H. (2003): Rate equations for non-convergent order-disorder processes – a review and application to orthopyroxene. *Eur. J. Min.*, **15**, 7–19.

Kroll, H., Lueder, T., Schlenz, H., Kirfel, A., Vad, T. (1997): The Fe^{2+},Mg distribution in orthopyroxene: A critical assessment of its potential as a geospeedometer. *Eur. J. Mineral.*, **9**, 705–733.

Kroll, H., Kirfel, A., Heinemann, R. (2006): Order and anti-order in olivine II: Thermodynamic analysis and crystal-chemical modelling. *Eur. J. Mineral.*, **18**, 691–704.

Le Hénaff, C., Hansen, N.K., Protas, J., Marnier, G. (1997): Electron density distribution in LiB_3O_5 at 293 K. *Acta Cryst.*, **B53**, 870–879.

McCoy, T. J., Keil, K., Clayton, R. N., Mayeda, T. K., Bogard, D. D., Garrison, D. H., Huss, G. R., Hutcheon, I. D., Wieler, R. (1996): A petrologic, chemical, and isotopic study of Monument Draw

and comparison with other acapulcoites: Evidence for formation by incipient partial melting. *Geochim. Cosmochim. Acta*, **60**, 2681–2708.

Morozov, M., Brinkmann, C., Kroll, H., Lottermoser, W., Tippelt, G., Amthauer, G. (2001): Mössbauer effect study of the Mg^{2+},Fe^{2+}-distribution in synthetic olivine (fa50 fo50). *Eur. J. Mineral.*, **13**, 127.

–,–,–,– (2002): Mg^{2+},Fe^{2+}-distribution in synthetic olivine ($Fa_{50}Fo_{50}$). Mineralogy for the New Millenium. 18th general meeting of the International Mineralogical Association. 1–6. September 2002, Edinburgh, Scotland. Programme with Abstracts, 86.

Morozov, M., Brinkmann, C., Lottermoser, W., Tippelt, G., Amthauer, G., Kroll, H. (2005): Octahedral cation partitioning in Mg,Fe^{2+}-olivine. Mössbauer spectroscopic study of synthetic $(Mg_{0.5}Fe^{2+}{}_{0.5})_2SiO_4(Fa_{50})$. *Eur. J. Mineral.*, **17**, 495–500.

Mueller, R.F. (1967): Model for order-disorder kinetics in certain quasi-binary crystals of continuously variable composition. *J. Phys. Chem. Solids*, **28**, 2239–2243.

– (1969): Kinetics and thermodynamics of intracrystalline distributions. *Min. Soc. America, Special Paper*, **2**, 83–93.

Pellas, P., Fiéni, C., Trieloff, M., Jessberger, E. K., (1997): The cooling history of the Acapulco meteorite as recorded by the ^{244}Pu and ^{40}Ar-^{39}Ar chronometers. *Geochim. Cosmochim. Acta*, **61**, 3477–3501.

Princivalle, F. (1990): Influence of temperature and composition on Mg-Fe^{2+} intracrystalline distribution in olivines. *Mineral. Petrol.*, **43**, 121–129.

Redfern, S.A.T., Artioli, G., Rinaldi, R., Henderson, C.M.B., Knight, K.S., Wood, B.J. (2000): Octahedral cation ordering in olivine at high temperature. II: An in-situ neutron powder diffraction study on synthetic $MgFeSiO_4$ (Fa50). *Phys. Chem. Minerals*, **27**, 630–637.

Rinaldi, R. Artioli, G., Wilson, C.C., McIntyre, G. (2000): Octahedral cation ordering in olivine at high temperature. I: In-situ neutron single-crystal diffraction studies on natural mantle olivines (Fa12 and Fa10). *Phys. Chem. Minerals*, **27**, 623–629.

Scheufler, C., Engel, K.V., Kirfel, A. (1997): An improved gas-stream heating device for a single-crystal diffractometer. *Journ. Appl. Cryst.*, **30**, 411–412.

Schmitt-Riegraf, C. (1996): Magmenentwicklung und spät- bis post-magmatische Alterationsprozesse permischer Vulkanite im Nordwesten der Nahe-Mulde. *Münster. Forsch. Geol. Paläont.*, **80**, 1–251.

Stimpfl, M., Ganguly, J., Molin, G. (2005): Kinetics of Fe^{2+}-Mg order-disorder in orthopyroxene: experimental studies and applications to cooling rates of rocks. *Contrib. Mineral. Petrol.*, **150**, 319–334.

Thompson, J.B. Jr (1969): Chemical reactions in crystals. *Am. Mineral.*, **54**, 341–375.

– (1970): Chemical reactions in crystals: Corrections and clarification. *Am. Mineral.*, **55**, 528–532.

Tribaudino, M. & Talarico, F. (1992): Orthopyroxenes from granulite rocks of the Wilson Terrane (Victoria Land, Antarctica): crystal chemistry and cooling history. *Eur. J. Mineral.*, **4**, 453–463.

Zema, M., Domeneghetti, M.C., Molin, G.M. (1996): Thermal history of Acapulco and ALHA81261 acapulcoites constrained by Fe^{2+}-Mg ordering in orthopyroxene. *Earth Planet. Sci. Lett.*, **144**, 359–367.

Received 16 July 2006
Modified version received 6 October 2006
Accepted 4 December 2006